AMAS WORKSHOP ON IMAGE ANALYSIS IN INVESTIGATION OF CONCRETE
SIAIC'02 – (PP.27–54) – WARSAW, OCTOBER 21-23, 2002.

2D - Image Analysis at the micro-scale in concrete research: applications and limitations

J. ELSEN

Katholieke Universiteit Leuven
Fysico-Chemische Geologie
Celestijnenlaan 200 C, B-3001 Heverlee
jan.elsen@geo.kuleuven.ac.be

1. Introduction

As a consequence of the widespread and increasing deterioration in concrete structures, research in durability of concrete has been conducted at a high priority level for the last 10 to 20 years. However, this research does not seem to have been conducted in parallel to the research in high performance concrete. As a result, severe deterioration may be observed in most concrete structures exposed to environmental conditions which could be harmful to concretes not absolutely durable. The main deterioration mechanisms are:

- frost/thaw action,
- alkali aggregate reactions,
- corrosion of reinforcement.

Micro-scale analyses using petrographic techniques have already been used in concrete technology for more than 20 years in Europe and has been proved to be a very important method for the quality control of recently cast concrete, for the inspection of concrete structures and for the investigation of concrete deterioration.

But, in a traditional petrographic analysis, the eye is used as a measuring instrument for the identification of the different components and for the recognition of structure phenomena of the material. The human visual system is extremely powerful in extracting interesting detail from an image but has limited capability in measuring quantitatively. As a consequence, a number of relevant parameters for the durability is determined qualitatively. This

means that a traditional petrographic analysis mainly consists in a subjective assessment of these important parameters, which is a serious limitation of this method. Several of those parameters can recently be quantified by image analysis methods, which replace traditional time consuming point counting techniques.

Concrete is composed roughly of about 75% coarse and fine aggregate (sand) and of 25% binder, commonly Portland cement, often mixed with blast furnace slag, silica fume, fly ash. The properties of concrete are, as it is for many materials, largely determined by its microstructure. Although concrete may appear to be a hard and impregnable material, it is in fact a porous material containing relatively soluble components. The pore size distribution in concrete covers 6 or 7 decades, ranging from 1 nm to 10 mm.

Traditionally, the pore size distribution is subdivided in three different pore classes [1]:

1. Gel pores with diameter < 50 nm (IUPAC-micropores and mesopores).
2. Capillary pores with diameter between 50 nm and 2 mm (IUPAC-macropores).
3. Air pores and cracks (compaction pores, entrained air pores, ...).

In Germany the capillary porosity is often subdivided in:

- Micro-capillary pores: $50\,\text{nm} \div 2\,\mu\text{m}$,
- Capillary pores: $2\,\mu\text{m} \div 50\,\mu\text{m}$,
- Macro-capillary pores: $50\,\mu\text{m} \div 2\,\text{mm}$.

The hydrated cement paste is described in the Powers-Brownyard model as a rigid gel sometimes called a xerogel (i.e. a gel from which the dispersion medium has been removed). In this model the hydrated cement paste is assumed to comprise three components from the volumetric standpoint: unreacted cement particles, hydration product and capillary pores. The gel pores correspond with the intra-granular porosity and the capillary pores correspond to the inter-granular porosity. The scheme presented in Fig. 1 summarises the pore sizes and the measurement methods.

The first and main difficulty for the interpretation of the measurement results is that the pore structure is often modified by the treatment before measuring (drying, degassing, ...) or during the measurement for example pore wall damage during mercury injection. Most of the results of the experimental methods are results for the dry material which is different from the real pore structure of concrete in situ. Some of the measurement techniques, however, allow to perform measurements in the presence of the liquid phase.

A second difficulty for the interpretation of the measurement results is that the porosity of mortar and concrete changes constantly in time. The

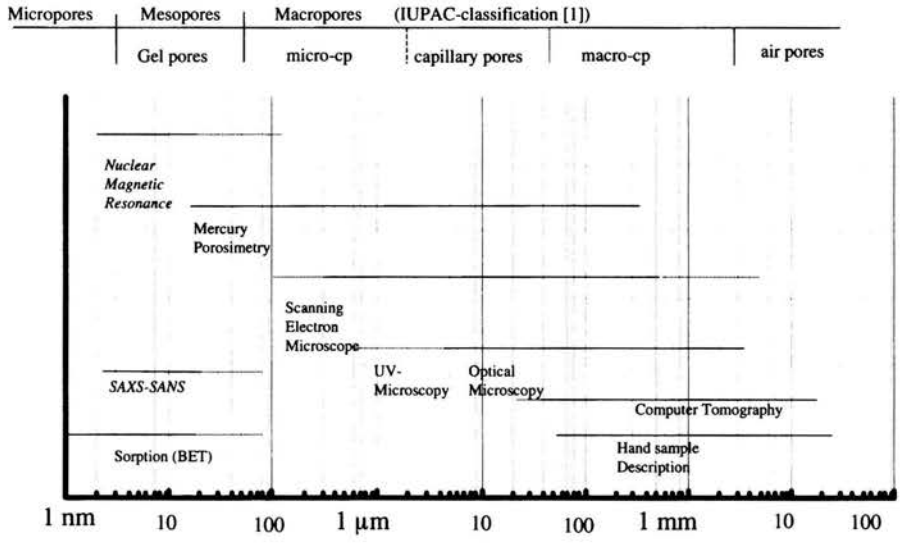

FIGURE 1. Pore size versus measurement method.

greatest changes occur during the first phase (days) of the hardening of the concrete, but other processes continue for years, for example carbonation, puzzolanic reactions etc.

A third difficulty is the heterogeneity of field concrete. One example of an heterogeneous microstructure is the higher porosity at the paste/aggregate interface, the so-called "auréole de transition".

The idea is to develop automated image analysis techniques into the petrographic analysis methods for monitoring and assessing the quality of concrete constructions and cementitious building materials. The following concrete characteristics which can be quantified by image analysis techniques will be described in more detail in the following chapters:

- Determination of the capillary porosity – w/c ratio.
- Determination of the air void content.
- Characterisation (SEM) of the microstructure of the cement paste – cement paste components and hydration degree.
- Quantitative characterisation of the presence and of the morphology of cracks and the development of methods to recognise, to describe and to quantify complex crack patterns.

2. Preparation of samples

Microscopic investigations are carried out on thin sections for optical microscopy and on polished sections for electron microscopy (SEM).

Thin sections

Thin sections are extremely thin slices with a thickness of 0.020÷0.030 mm, so thin, that they have become transparent for light. Moreover the finest pores are impregnated with a dye-containing resin, making it possible to make the fine cracks and pores light up by means of an exciting UV light beam. The preparation of fault free thin sections with a constant and homogeneous thickness, requires precision work. The first step in manufacturing thin sections is the reduction of the sample to a small block of for example 30 × 50 × 20 mm. Then this prism is impregnated under vacuum with a low-viscous resin. This resin contains a fluorescent dye. After the hardening of the epoxy resin one side of the block is carefully ground and then glued to a glass plate. Afterwards the thickness of the block is reduced, first by sawing off the material which sticks out more than half a millimetre above the glass plate, and then by grinding or polishing the material in different steps until the desired thickness of 0.020÷0.030 mm is obtained. Finally the thin section is covered with a cover glass.

The fluorescence allows the lighting-up of the cracks and pores filled with the fluorescent resin, by aiming an exciting light ray produced by a band-pass filter on to the thin section. The fluorescent particles in the sample are excited by the selected light ray and thereby themselves emit a fluorescent light ray. On the other hand the parts in the sample without the fluorescent resin do not light up and remain dark. The fluorescent light ray is finally selectively let through by a stop-filter for optimal observation.

Polished sections

The pore structure and phase composition of the samples can also be measured on polished sections using a scanning electron microscope (SEM). The samples are firstly impregnated under vacuum with a fluid epoxy before polishing. The images are obtained on these polished sections (5 × 3 cm) with a SEM using a solid state Back-Scattered Electron detector (BSE). Chemical Image mappings are images based on the information recorded and digitised from Energy-Dispersive X-Ray analysis (EDX) detectors. The examination by microscopy of polished specimen of porous materials is facilitated if the pores are filled with a hard material such as an epoxy resin. The resin serves to stabilise the microstructure and provides a support to prevent damages

during polishing and microcracking during the SEM investigation. The resin, due to its low average atomic number, may also improve the identification of pores using scanning electron microscope (SEM) with backscattered electron imaging (BEI). The method, commonly used to achieve the filling of the pores by an epoxy resin, is the following one; first, the sample is dried under vacuum, then, while under vacuum, the dried sample is immersed in the epoxy resin and finally, the pressure is brought back to the atmospheric pressure while the sample is still immersed in the resin. This method presents a major problem: the sample is dried and it is well known that drying causes shrinkage and microcracking. This phenomenon is mainly due to the capillary forces which appear at the interface liquid-solid.

An alternative procedure, used for preparing biologic samples [2, 3] has been proposed to avoid this problem. This procedure involves two steps:

1. first, replacing pore-water with ethanol,
2. then replacing ethanol with epoxy.

The method requires to keep the samples in water before starting the impregnation procedure. The sample is generally a thin slice in order to save resin and to improve its penetration. All grinding have to be done dry because alcohol-based-lubricants can soften the resin and after a prolonged contact lift the resin from the voids. During grinding, the paste appears much smoother and highly reflective. The last step is to clean the surface of the sample to remove powdered materials. The specimen is placed in a container filled with ethanol and the container in an ultrasonic bath for about ten seconds. Finally, the specimen is rinsed and dried with forced air.

The polishing procedure is a three step process: polishing, cleaning, examination.

This process can be repeated as long as necessary and several grades of diamond polishing paste are used. The specimens are polished in a direction opposite to the wheel rotation and the propylene glycol is used as a polishing lubricant. During the process, the specimens are examined under a binocular microscope for evaluation of the polished surface.

3. Use of image analysis techniques

3.1. Measurement of the capillary porosity – w/c ratio

3.1.1. Introduction. The w/c ratio is one of the most important parameters in concrete technology not only because of its direct relation with concrete strength but also because of its importance with regard to the durability of the concrete. This is due to the direct relationship between the w/c ratio and the capillary porosity of the cement paste. A higher capillary porosity

results in a higher permeability towards aggressive agents such as noxious liquids and gases. Therefore, the determination of the w/c ratio of hardened concrete is of prime importance for deterioration diagnosis as well as for concrete Quality Assurance in general. An optical method to determine the w/c ratio of hardened concrete using thin sections has been developed in Denmark [4] and is used nowadays generally in Denmark and the Scandinavian countries [5]. This method is based on the principle that the intensity of the fluorescence of the epoxy in the cement paste is proportional to the capillary porosity. The higher the fluorescence intensity is, the higher the capillary porosity and the w/c ratio are. The fluorescence intensity of thin sections prepared from concrete samples with an unknown w/c ratio are visually compared with a reference series of thin sections of a concrete with a known w/c ratio, a well-defined cement, and a curing under standard conditions for 28 days. The first results of quantitative measurements of w/c ratio were published by Mayfield [6] on polished specimen using a photodiode. Quantitative results using image analysis techniques were published by Wirgot and Van Cauwelaert [7]. They concluded that the fluorescence of impregnated cement paste can be measured with image analysis techniques coupled with a statistical analysis of the data. The precision was estimated as being insufficient.

The objective of research carried out as a EC-BRITE project was the development of an automated image analysis procedure to determine the w/c ratio optically from fluorescent dye impregnated thin sections of concrete and the results were published in 1995 [8].

3.1.2. Image Analysis Procedure. Four different image analysis methods have been evaluated: an interactive method, an automated method with thresholding of grey values by the operator, an automated method using fixed threshold values, and a fully automated method without thresholding.

The final measurement values given further on in this paper have been obtained by the fully automated method without thresholding for the cement paste samples and by the automated method using fixed threshold values for the concrete samples.

Interactive method

On the digitized image, the areas in the cement paste to be evaluated are interactively defined by the operator. The distribution of grey values of each selected area is measured and the mean grey value of each area is considered as a measure for the fluorescence intensity of that area. The measured w/c ratio is calculated as the mean of the weighted mean grey

values of the selected areas. The main disadvantages of this method are that the relevant areas have to be defined interactively by the operator for each image making this procedure time consuming in regard to man-hours. A second disadvantage is that this method is not highly reproducible. The areas examined are interactively defined and thus influenced by the subjectivity of the operator. If for example, very homogeneous areas are always chosen by the operator, then the results will not be truly representative for the sample.

However, this method is very useful for measuring the w/c ratio of a concrete for which it is very difficult to identify the cement paste automatically. This is the case for example for a concrete with an extremely high air content, or with a very high content of porous aggregates.

Fully automatic method

In the fully automatic method, a thin section is scanned and the complete grey level histogram of each image is accumulated and stored (see Fig. 2).

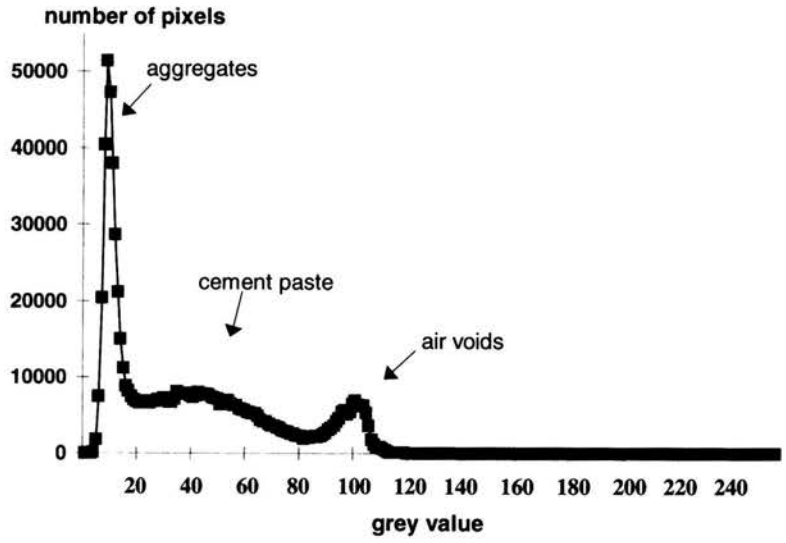

FIGURE 2. Complete grey level distribution of a thin section prepared out of a concrete reference sample.

The complete grey level distribution exhibits the following features:

- a considerable portion of the concrete samples consists of opaque material which results in a strong peak at low grey-values,
- at the high grey levels there is a peak due to porosity,

- a broad distribution of grey levels in between is due to the cement paste fluorescence.

However, the strong peak at low grey-values is not caused by the aggregates only. It can be very easily determined by visual observation using the microscope that a portion of the unhydrated cement particles are as dark as the aggregate grains. This implies that it is not possible to measure a thin section of concrete automatically with the complete grey level distribution and to pick out afterwards the cement paste grey level distribution very accurately.

The main conclusion of the measurements with this method is that it is not possible to select the cement paste area with the fully automatic method without loosing the black unhydrated cement particles. The method is very rapid, has a high repeatability but gives inaccurate results for concrete but is very useful for cement paste samples.

Automated method with thresholding of grey values by the operator

In an automated measurement with thresholding a series of parameters are defined at the start of the measurement by the operator. The grey level thresholds for the selection of the cement paste are selected by the operator and, if necessary, all images are rapidly scanned to skip eventually all images which could give wrong results due to preparation errors, porous aggregates etc. After these initial operations, the measurements are performed automatically. This method is rapid and gives good results for cement paste and concrete samples, but has a low multi-operator precision (repeatability).

Automated method using fixed threshold values

After initialisation of the measurement setup , all images are rapidly scanned to skip eventually all images which could give wrong results due to preparation errors, porous aggregates etc. After these initial operations, the measurements are performed automatically.

The following equipment has been used:

- optical research microscope (ZEISS Axioplan),
- scanning stage (MARZHAUSER),
- microscope control processor (MCP-KONTRON Elektronik),
- image analysis system (IBAS system, KONTRON Elektronik),
- a black and white CCD-camera (KAPPA CF 8/1) with the following characteristics:

- a high sensitivity to light (0.12 lux),
- an automatic or manual gain control,
- a resolution of 752 TV lines (752 (H) and 582 (V) picture elements).

Measurement conditions:

- Epi-fluorescence – objective: 10× and Optovar-1.25.
- filter set: BP 450-490 / LP515.
- camera gain: Stored Manual Mode.
- scale factor: 1 pixel = 1.20 × 1.24 micron.
- area of one image: 648.1 × 673.7 micron.
- number of images measured: 15 × 12 = 180.

A grid of 1080 images is defined over the thin section, 45 in the X-direction and 24 in the Y-direction. Every third image in the X-direction and every second image in the Y-direction is considered in a systematic sampling plan, i.e., a total of 180 images are considered. The total area considered is thus 648 micron × 674 micron × 15 × 12 or 78.6 mm^2.

Initialisation:

- The grey level measurement is calibrated on a reference thin section prepared from a block of pure fluorescent epoxy. The illumination of the microscope lamp is always kept at its maximum intensity and a mean grey value of the reference thin section is adjusted to a predefined value of 200 ± 3 by changing the gain of the camera.
- All images can rapidly be scanned and the operator can skip those images which would give obviously wrong results. Wrong results can be obtained due to porous aggregates and to preparation defects.
- A shading correction can be applied.
- The area considered and the area measured can interactively be chosen by the operator.

A series of parameters are defined at the start of the measurement by the operator. The grey level thresholds for the selection of the cement paste are fixed values. After these initial operations, the following steps are performed automatically:

1. The incoming video signal is integrated in four steps (sequence of TV cycles). This is used to improve the signal/noise ratio of an image.
2. Very small objects are eliminated on the basis of their area, in pixel units by a scrap command. A second scrap command is used to include

the unhydrated cement particles in the phase which will be measured. These particles cannot be selected by their grey values.

3. All isolated particles (holes) inside the aggregate grains are filled.
4. Three erosions are being applied to the image with an octagon structuring element. This is used to correct for the halo around the air voids, and to correct the rim around aggregates more precisely in thin sections with a low w/c ratio.

3.1.3. Measurement results of the cement paste reference samples

Series 1A: Pure cement paste samples (CP) with OPC-cement (Belgian - CEM I; P40).

Series 1B: Pure cement paste samples (CP) with slag-cement (Belgian - CEM III; HK40).

The measurement on cement paste samples is much more straightforward because of the absence of any aggregates. The lower-limit for the grey values has always been set to zero for the measurements shown in Tables 1 and 2 and Fig. 3. The upper-limit threshold value has been kept constant.

TABLE 1.

Sample code	Cement type	w/c ratio	Mean grey level
CPa-I-1	CEM I	0.25	71.3
CPa-I-2	CEM I	0.33	89.5
CPa-I-3	CEM I	0.50	109.8
CPa-I-4	CEM I	0.60	122.5
CPa-III-1	CEM III	0.25	50.2
CPa-III-2	CEM III	0.33	82.1
CPa-III-3	CEM III	0.50	125.8
CPa-III-4	CEM III	0.60	138.8

Influence of the maturity of the samples

The influence of the maturity of the samples after 28 days has been investigated. Thin sections have been prepared from the CPa-I series after one, two and three years. and from the CPa-III series after 4 months. The results of the investigation indicated the following:

- Varying the maturity of the cement paste samples with CEM-I type between 28 days and 3 year does not have a significant influence on the measured effective w/c ratio.

TABLE 2.

Sample code	Cement type	w/c ratio	Mean grey level
CPb-I-1	CEM I	0.35	71.5
CPb-I-2	CEM I	0.40	85.5
CPb-I-3	CEM I	0.45	104.5
CPb-I-4	CEM I	0.50	113.2
CPb-I-5	CEM I	0.55	143.0
CPb-I-6	CEM I	0.60	155.5
CPb-I-7	CEM I	0.70	144.0

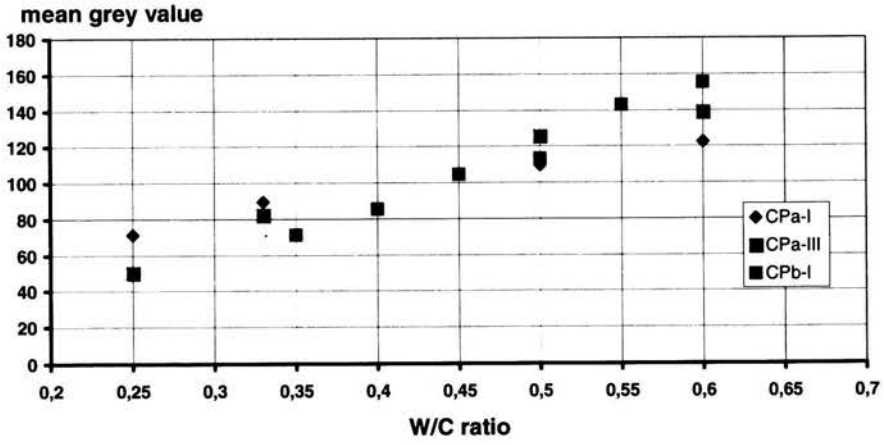

FIGURE 3. Mean grey value for the reference pure cement paste samples as measured with automated image analysis techniques.

- Varying the maturity of the cement paste samples with CEM-III type between 28 days and 4 months does have a significant influence on the measured effective w/c ratio (Table 3).

TABLE 3.

Sample code	Cement type	w/c ratio	Mean grey level	
			28 days	4 months
CPa-III-1	CEM III	0.25	50.2	41.7
CPa-III-2	CEM III	0.33	82.1	70.3
CPa-III-3	CEM III	0.50	125.8	83.8
CPa-III-4	CEM III	0.60	138.8	111.4

3.1.4. Measurement results of the concrete samples

Series 2A: Reference concrete samples (C) with OPC-cement (Danish - CEM I).

The results of the measurements for the concrete samples are shown in Table 4 and Fig. 4. These samples have been measured with fixed threshold values.

TABLE 4.

Sample code	Cement type	w/c ratio	Mean grey level
Ca-I-1	CEM I	0.35	48.2
Ca-I-2	CEM I	0.40	56.3
Ca-I-3	CEM I	0.45	68.4
Ca-I-4	CEM I	0.50	75.9
Ca-I-5	CEM I	0.55	86.7
Ca-I-6	CEM I	0.60	92.3
Ca-I-7	CEM I	0.70	101.9

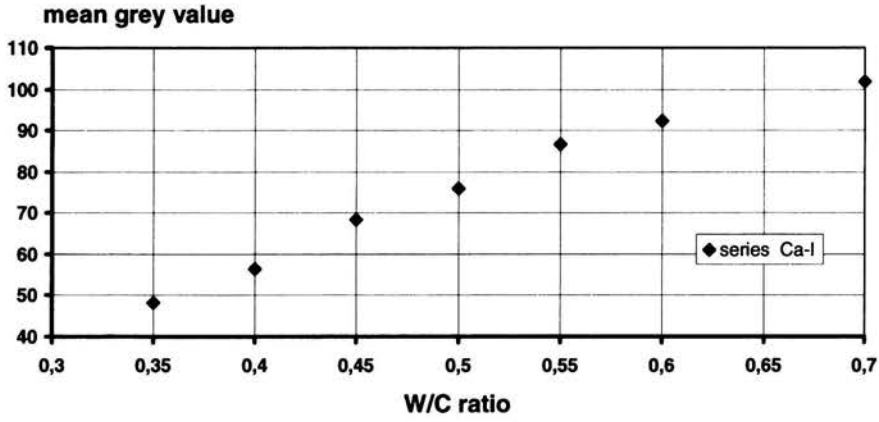

FIGURE 4. Mean grey value for the thin sections of the seven concrete reference samples of series 2A, as measured with automated image analysis techniques.

Series 2B: Reference concrete samples (C) with OPC-cement (Danish - CEM I).

To investigate the validity of the measurement 10 different concrete mixes have been prepared in laboratory conditions. Cubes of 158 mm were prepared

from each concrete mix. These samples are summed up in Table 5. One half of the samples has an unknown w/c ratio. This w/c ratio is only known by the responsible of the concrete laboratory. Thin sections of these samples have been prepared and Image Analysis measurements have been performed.

TABLE 5.

Sample code	Cement type	w/c ratio	Mean grey value
Cb-I-1	CEM I-42.5	0.35 – known	57.6
Cb-I-2	CEM I-42.5	0.40 – known	61.0
Cb-I-3	CEM I-42.5	0.45 – known	72.1
Cb-I-4	CEM I-42.5	0.50 – known	84.3
Cb-I-5	CEM I-42.5	0.60 – known	96.0
Cb-I-6	CEM I-42.5	unknown – 0.37	55.4
Cb-I-7	CEM I-42.5	unknown – 0.47	79.1
Cb-I-8	CEM I-42.5	unknown – 0.55	91.5
Cb-I-9	CEM I-42.5	unknown – 0.65	100.4
Cb-I-10	CEM I-42.5	unknown – 0.70	92.1

3.1.5. Influence of the type of illumination used. The influence of the type of illumination used has been investigated on the cement paste reference samples (series 1).

There are two types of illumination for Fluorescence Microscopy (FM): transmitted and incident illumination. For both types of illumination an excitation filter is used to select the appropriate excitation wavelengths from the light emitted by the light source. The fluorescence specimen is illuminated and a barrier filter is used to separate emitted light from unabsorbed exciting light.

- *Transmitted light illumination*
  This type of set-up is the earliest applied method of FM. The condenser focuses the exciting light on to a microscopic field. The emitted fluorescence is collected by the objective and observed through an eyepiece. Essential to this configuration is that two different lenses are used to focus the exciting light and to collect the emitted light.
- *Incident light illumination (EPI-illumination)*
  This configuration is based on the adaptation of the vertical illuminator used in reflection microscopy and was developed more recently. In this set-up there is only one lens for focusing exciting light on to the specimen and collecting emitted light from the fluorescing specimen. In order to separate fluorescence emitted light from unabsorbed exciting

light in a special type of mirror, a chromatic beam splitter is positioned above the objective. Finally a barrier filter is needed to eliminate any residual exciting light.

The configuration with transmitted light illumination has several disadvantages compared to the set-up of the incident type of illumination [9]. For this reason we decided to choose a configuration with EPI-FM on our optical microscope. Because of discussions about the validity of using one or the other configuration for this specific application, we have prepared a set-up on an optical microscope which is capable of using both types of illumination. With this set-up we have measured firstly a thin section using transmitted illumination and thereafter measured the same images of the same sample using incident illumination.

TABLE 6.

Sample code	w/c ratio	Mean grey level	
		transmitted illumination	incident illumination
CP1	0.25	28.08	39.68
CP2	0.33	41.72	59.49
CP3	0.50	65.47	87.01
CP4	0.60	71.92	95.05

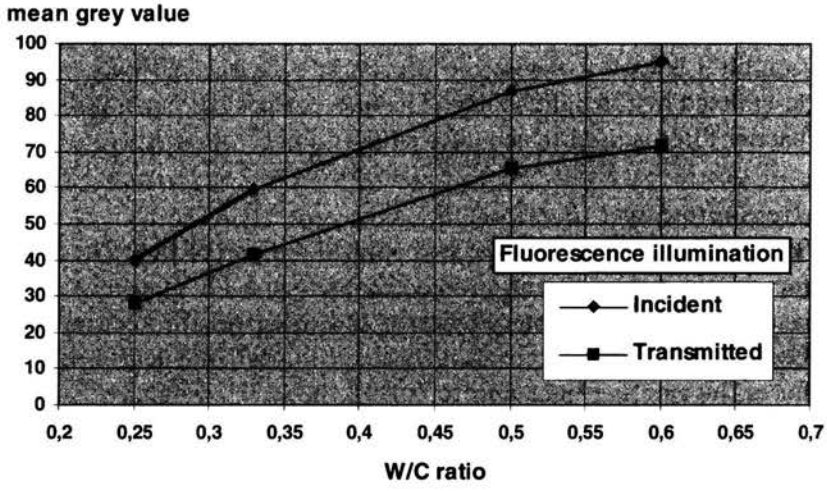

FIGURE 5. Mean grey value for the thin sections of four cement paste samples as measured with automated image analysis techniques using transmitted and incident illumination conditions.

The thickness of the thin section will highly influence the intensity measurement of the fluorescence when using the transmitted light configuration. If the thickness of the thin section exceeds a certain limit, the cement paste will appear too dark as the large thickness will impede the penetration of the UV-light.

The measurements were carried out on the cement paste samples (CP) and the results are shown in Table 6 and Fig. 5. The upper-limit threshold value was always kept constant.

3.1.6. Evaluation of the method and conclusions. The measurements on the pure cement paste samples confirm the direct relationship between the w/c ratio of the samples and the mean grey value measured on thin sections.

Both transmitted and incident illumination can be used for this measurement, but the transmitted illumination is more sensitive to differences in thickness of the thin section.

The results of the measurements on the thin sections prepared out of the reference concrete series also indicate a clear relationship between the w/c ratio and the mean grey value but these measurements indicate that the effective w/c ratio measured is influenced by other parameters related to the aggregate fraction present in the concrete

The main difficulty of measuring the fluorescence intensity of the cement paste phase in concrete samples automatically, is that we need to include the unhydrated cement particles within this phase. In our measurement procedure , the unhydrated particles are included in the cement phase for each image separately by image analysis processing techniques. The grey level distribution of the complete cement paste phase is then measured automatically.

All the measurements here have been performed for cement paste and concrete samples which have been cured under laboratory conditions for 28 days. The results cannot of course be transferred in a simple way to field concrete. For damage diagnosis this method must be used with great care especially for concrete samples prepared with other than CEM-I type cement and for samples with less-known aggregate types.

3.2. Air voids[1)]

3.2.1. Introduction. It is generally recognised that the air void structure of concrete is a critical parameter for the durability of concrete subjected to frost/thaw action and de-icing salts. An air void analysis is the only method available on hardened concrete to evaluate the air void structure of concrete.

[1)] Part of the results presented in this Section have been published by J. Elsen (2001) in [10].

Traditionally the air void system is characterised and assessed in terms of the total air content and the spacing factor of the air bubbles as defined by Powers [11]. More recently the micro air content (A300) has been recognised to be also an important factor [12]. For ordinary concrete, a great number of test results are available which document the correlation between the frost/thaw resistance of the concrete and the spacing factor of the air bubbles, whereby a spacing factor of about 0.200 mm seems to guarantee a good frost resistance [13]. General relationships of the different parameters of the air void system and the parameters having an influence on the stability of the air void system have been extensively investigated, especially at Laval University, Quebec [14]. More detailed information about the different measurement methods can be found in Elsen et al. [15].

Automated methods for air void analysis using Image Analysis (IA) techniques improve the existing methods by reducing the measurement time from 4-6 hours manually to 10-30 minutes. Area and diameter measurements can be performed using these automated measurements making it possible to quantify the spacing between the air voids more precisely. Limited information although is available concerning the precision of the air void measurement methods. Most articles that have been published about the precision of air void analysis measurements including results from interlaboratory measurements present only data obtained microscopically using the traditional manual methods, e.g. Langan and Ward [16], Pleau and Pigeon [17] and Sommer [18].

A limited number of experimental results of air void measurements using automated systems have been published by individual laboratories [19, 20]. Automated systems use automated traverse methods or Image Analysis methods. The calculations in the former case do not differ from the manual linear traverse method because both methods measure the individual chord lengths. The latter methods using Image Analysis techniques are not only capable of measuring chord lengths but also diameters, section areas and the perimeters of the air voids.

A comparison of the automated method versus traditional manual method has been published by Ohta et al. [21]. They found a reduction of measurement time with 83-88% and a reduction of the coefficient of variance of the measurement of 75% using an automated method.

3.2.2. Standardisation and measurement methods. The air void system (ASTM C457-90, EN480-11) is most often characterised and assessed in terms of the total air content, the micro air content, the specific surface and the spacing factor of the air bubbles.

Total air content (physical parameter), symbol A%.

The total air content is the proportion of volume of air voids to the total volume of concrete, expressed as a percentage by volume.

Micro air content (physical parameter), symbol A300.

The micro air content is defined as the air content of air voids of 0.3 millimetre diameter or less.

Specific surface (physical parameter), symbol α.

The specific surface is a calculated parameter representing the total surface of all voids divided by the total volume of voids, in mm^{-1}.

Spacing factor (hypothetical parameter), $\bar{L}$

The spacing factor is defined by T.C. Powers [1] as a parameter related to the maximum distance of any point in the cement paste from the periphery of an air void:

$$\bar{L} = \begin{cases} \dfrac{p}{A\alpha} & \text{for } A \leqslant 4.342, \\ \dfrac{3}{\alpha}\left[1.4\left(\dfrac{p}{A}+1\right)^{\frac{1}{3}} - 1\right] & \text{for } A > 4.342, \end{cases}$$

where:
$\bar{L}$ is the spacing factor [mm],
p is the paste content [%],
A is the air volume content [%],
α is the specific surface [mm^{-1}].
$\bar{L}$, A and α are not independent parameters. Therefore the spacing factor will not be treated further here in this article as this spacing factor results from a calculation with the paste content, the air content and the specific surface as input.

ASTM C457-90

Total air content and the spacing factor or the specific surface of the air bubbles are traditionally determined world-wide following ASTM C457 wherein a manual method is described using either a point count or a linear traverse method (Rosiwal-method). These measurements are made on finely ground sections of the hardened concrete mounted under a microscope. The air void structure is examined by scanning along a series of traverse lines.

EN480-11

Recently, the new European standard EN480-11 "*Admixtures for concrete, mortar and grout; Test methods: Determination of air void characteristics in hardened concrete*" has been adopted.

The major differences between these two standards are summarised in Table 7.

TABLE 7. Comparison between EN480-11 and ASTM C457-90.

Parameter	EN480-11	ASTM C457-90
Method	Linear traverse method	A: linear traverse method B: modified point count method
Area (max. aggregate 31.5 mm or 37.5 mm respect.)	150 mm^2	155 mm^2 (= 24 in^2)
Number of specimens	2	$\geqslant 1$
Length of traverse line (max. aggregate 31.5 mm or 37.5 mm respect.)	$\geqslant$ 2400 mm	$\geqslant$ 2540 mm (= 100 in)
Magnification of the microscope	100× ± 10×	50× to about 125×
Air void size distribution	yes	no
Micro air content	yes	no

3.2.3. Round robin test. A round robin test has been held on nine concrete samples. Nine concrete mixes were prepared by one of the participants of the intercomparison test taking care to cover the whole range of air void content and specific surface currently found in practice. Specimen with dimensions 10 × 10 × 2 cm were prepared out of these 9 concrete bodies. These 9 samples were polished and measured by the seven laboratories using a manual air void analysis method. The samples were thereafter in a second step prepared for the automated air void analysis measurements. The samples have been contrast enhanced so that the air voids can easily be selected from the cement paste and the aggregates. After being prepared in this way, the samples have been measured by the six laboratories using automated air void analysis measurement systems. The paste content for the nine samples involved was as follows:

Sample	1	2	3	4	5	6	7	8	9
Paste content [%]	26.0	26.0	26.5	26.5	26.5	26.5	24.1	24.1	27.3

3.2.4. Results. The summary of the results of the round robin measurements results are presented in Table 8. Thirteen participants (C1,...,C13) have measured the same nine samples for air void content, for specific surface and for the spacing factor.

3.2.5. Statistical evaluation

Z-score

The results were converted to Z-scores to be able to study the interrelationships in the data by neutralizing the influence of the specifics of the nine samples used in the round robin experiment. The differences, perceived in these converted data, should then be due to the round robin participants and not a result of some specific property of the samples being analyzed. This transformation has the following form:

$$Z_{ij} = \frac{\text{row}_{ij} - \text{mean(row)}}{\text{stdev(row)}}.$$

The original matrix of 9 samples has different row average values and standard deviations. The Z-score transformation changes it into a matrix that has rows with the mean value of 0 and standard deviation of 1.0. The Z-scores are presented in a tabular fashion in Table 9 and 10. Note that the columns of the matrix have been reordered to bring together participants of the same type of equipment: "A" stands for automatic, "P" for point-count measurement instruments and "R" for Rosiwal-type (i.e. linear-traverse) instruments.

To allow uncluttered assessment of the quality of results, the Z-scores have been averaged across the 9 samples, giving one single Z-score for every participant in the experiment (Table 11). A scattergram of the mean Z-scores of the specific surface (α) versus the air content (A) (Fig. 6) indicates that the measurements are not a homogenous sample.

Two cases at the top of Fig. 6 exhibit behaviour, which is significantly different from the rest of the group. Note that they belong to different measurement methods. One is using the automated and one the Rosiwal-traverse measurement method. The data set (Table 8) has been evaluated for the presence of outliers following the Dixon Q-test (ISO 5725: *Precision of test methods – Determination of repeatability and reproducibility for a standard test method by interlaboratory tests – 13 Dixon's test*). No outlier values were found for the air content values (95% confidence interval). If we perform this Q-test for the specific surface results, 2 of the 9 results of C10 and 2 of the 9 results of C04 are evaluated as being outliers.

TABLE 8. Summary of results of measurements of Round Robin Test.

Laboratory	C01	C02	C03	C04	C05	C06	C07	C08	C09	C10	C11	C12	C13
Method used*	A	R	P	A	A	R	R	P	P	R	A	A	A
Sample	Air volume content (A [%])												
1	2.4	2.6	3.1	3.6	2.5	3.0	3.0	3.4	2.6	1.7	2.3	2.7	2.5
2	3.9	3.9	3.9	4.8	3.5	4.0	4.0	3.9	3.1	2.7	4.5	3.2	3.7
3	12.3	11.1	13.0	13.1	14.2	8.8	13.8	12.1	11.8	10.3	13.4	13.8	11.4
4	0.9	1.5	1.7	1.1	1.3	1.5	1.3	1.6	1.0	1.2	1.2	1.9	1.1
5	7.9	7.9	9.7	9.6	8.6	8.1	9.3	9.1	7.8	6.4	9.8	7.7	8.4
6	4.8	4.9	4.6	5.7	4.8	4.7	5.4	6.9	3.9	3.5	5.8	5.8	5.3
7	8.9	7.3	6.2	6.8	9.1	5.9	9.3	9.1	10.1	6.9	8.3	9.3	8.6
8	9.0	8.3	9.5	7.9	9.4	7.0	9.1	9.0	9.3	8.5	8.6	8.5	8.2
9	1.3	1.0	0.9	1.0	1.3	1.4	1.6	1.5	1.6	1.0	1.2	1.4	1.4
Sample	Specific surface (α [mm^{-1}])												
1	38	47	36	53	42	42	50	44	42	62	40	40	42
2	45	39	40	47	42	37	42	43	44	58	43	44	44
3	42	40	39	47	36	38	47	39	40	56	33	39	42
4	14	18	16	45	12	18	23	15	11	21	18	22	14
5	29	34	30	38	28	26	37	30	31	50	31	33	30
6	28	34	38	41	27	27	39	25	33	45	31	33	27
7	16	18	18	24	16	21	18	15	12	30	22	22	18
8	21	23	19	29	20	25	25	22	19	28	27	27	22
9	11	20	16	54	11	22	22	12	6	23	17	18	12

* A = Automated, P = Manual Point Count, R = Manual Traverse (Rosiwal).

TABLE 9. Z-scores for air volume content (A).

Sample	C1	C4	C5	C11	C12	C13	C3	C9	C8	C2	C6	C7	C10
1	-0.65	1.76	-0.45	-0.85	-0.05	-0.45	0.76	-0.25	1.36	-0.25	0.56	0.56	-2.05
2	0.22	1.83	-0.49	1.29	-1.03	-0.14	0.22	-1.21	0.22	0.22	0.40	0.40	-1.92
3	0.04	0.55	1.26	0.74	1.00	-0.54	0.49	-0.28	-0.09	-0.73	-2.20	1.00	-1.24
4	-1.47	-0.79	-0.11	-0.45	1.95	-0.79	1.26	-1.13	0.92	0.58	0.58	-0.11	-0.45
5	-0.59	1.08	0.12	1.34	-0.79	-0.08	1.24	-0.69	0.63	-0.59	-0.39	0.83	-2.11
6	-0.32	0.70	-0.32	0.81	0.81	0.24	-0.55	-1.34	2.06	-0.21	-0.44	0.36	-1.80
7	0.56	-0.99	0.71	0.12	0.86	0.34	-1.43	1.45	0.71	-0.62	-1.65	0.86	-0.91
8	0.52	-1.06	1.09	-0.06	-0.20	-0.63	1.24	0.95	0.52	-0.49	-2.35	0.66	-0.20
9	0.10	-1.16	0.10	-0.32	0.52	0.52	-1.58	1.35	0.93	-1.16	0.52	1.35	-1.16
Type	A						P			R			

TABLE 10. Z-scores for specific surface (α).

Sample	C1	C4	C5	C11	C12	C13	C3	C9	C8	C2	C6	C7	C10
1	-0.92	1.21	-0.35	-0.63	-0.63	-0.35	-1.20	-0.35	-0.07	0.36	-0.35	0.79	2.49
2	0.26	0.66	-0.34	-0.14	0.06	0.06	-0.73	0.06	-0.14	-0.93	-1.33	-0.34	2.84
3	0.11	0.96	-0.92	-1.44	-0.41	0.11	-0.41	-0.24	-0.41	-0.24	-0.58	0.96	2.50
4	-0.58	3.01	-0.81	-0.12	0.35	-0.58	-0.35	-0.93	-0.46	-0.12	-0.12	0.46	0.23
5	-0.62	0.84	-0.79	-0.30	0.02	-0.46	-0.46	-0.30	-0.46	0.19	-1.11	0.67	2.78
6	-0.79	1.23	-0.95	-0.30	0.02	-0.95	0.82	0.02	-1.27	0.18	-0.95	0.98	1.95
7	-0.70	1.04	-0.70	0.60	0.60	-0.27	-0.27	-1.57	-0.92	-0.27	0.38	-0.27	2.34
8	-0.76	1.56	-1.05	0.98	0.98	-0.47	-1.34	-1.34	-0.47	-0.18	0.40	0.40	1.27
9	-0.66	2.99	-0.66	-0.15	-0.07	-0.57	-0.23	-1.08	-0.57	0.10	0.27	0.27	0.36
Type	A						P			R			

TABLE 11. Across-samples means of Z-scores.

Sample	C1	*C4*	C5	C11	C12	C13	C3	C9	C8	C2	C6	C7	*C10*
Type	A						P			R			
A	-0.18	*0.21*	0.21	0.29	0.34	-0.17	0.18	-0.13	0.81	-0.36	-0.55	0.66	*-1.92*
α	-0.52	*1.50*	-0.73	-0.17	0.10	-0.39	-0.46	-0.64	-0.53	-0.10	-0.37	0.44	*1.86*

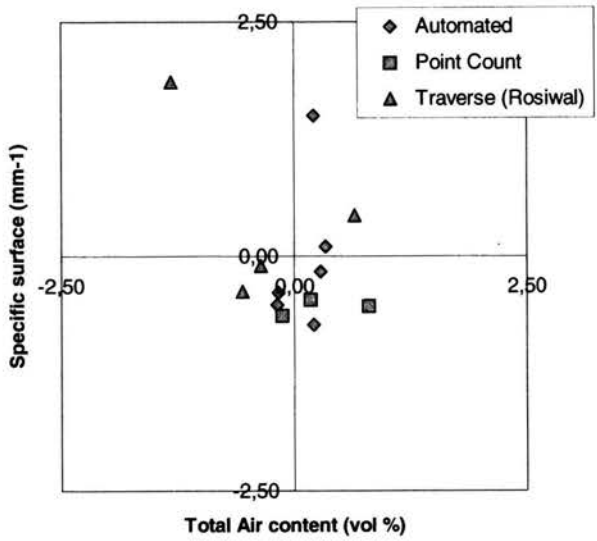

FIGURE 6. Plot of the mean Z-score for specific surface (α) against the mean Z-score for total air content (A). The 13 laboratories used an automated or point count or Rosiwal-traverse method.

Sampling variability

In search of possible sources for the variance between the different cases in the round robin experiment, the issue of the influence of sampling on the measurement has to be addressed. By calculating the values for the expected variability using 2400 mm for total traverse and the group averages for air volume content and specific surface, than on average the sampling variability contributes 86% to the air volume percent and 60 % to the specific surface variability in our measurements.

3.2.6. Conclusions. A round robin test has been held on nine concrete samples covering the whole range of air void content and specific surface currently found in practice. Thirteen laboratories in Europe participated to the intercomparison test of which six used an automated method and seven a manual method for air void analysis. Three out of these last seven laboratories use a manual point-count method and the other four laboratories use a manual linear traverse (Rosiwal) method.

The results indicate that the method used did not seem to have a significant influence on the results and that, excluding two outliers, they all lie within the sampling error to be expected on the basis of standard requirements. The results obtained by automated measuring methods all lie statis-

tically in the group of all measurement results, a statistical analysis points out that sampling is the major reason of variation for air void analysis.

The automated methods are very fast but they can be problematic when a high amount of porous sand grains is present in the concrete. A second disadvantage of these automated methods is that it is not possible with the current methods being used to measure the paste content of the sample in an automated way. Furthermore for these automated methods it became clear that sample preparation is of crucial importance for obtaining reliable and comparable results. Therefore, detailed guidelines describing sample preparation have been produced before the intercomparison testing programme. The repeatability of the Rosiwal traverse method using automated image analysis techniques has been evaluated in one laboratory by repeated measurements (10) performed on 15 samples. A mean coefficient of variation of 3.01% has been found for total air content with a standard deviation of 1.54, and of 3.48% with 1.89 as standard deviation for the specific surface of the air voids.

3.3. Quantitative characterisation of cracks and crack patterns

Image Analysis procedures for crack analysis have been developed by different research groups in the past, mostly based on quantitative image analysis of polished sections of hardened concrete samples. But the information available therefore is two-dimensional. To obtain information of the three dimensional character statistical-geometrical relationships have often been applied provided by stereology. One of the classical methods in stereology proposed by Saltykov is based on a coverage of the sample by a line-grid. The basic idea is to count the number of intersections between the crack network and the template. It is possible to derive from these measurements the following characteristic parameters for the crack network: total crack length per unit sample area, degree of orientation, specific surface area, mean free path, etc.

A new technique to obtain the three-dimensional information is the use of microfocus X-ray computer tomography (22). X-ray computer tomography (CT) is a technique which allows to reconstruct the 3D internal structure of objects non-destructively without any prior preparation, by acquiring radiographic projections from many different viewing angles from 0 to 180 degrees. Each of the recordings is fed into a computer. From these projections the 3D structure of the object can be calculated using a reconstruction algorithm.

Recently, there has been a significant improvement in the development of X-ray microscopes using synchrotron sources. However, these facilities are rather complicated and expensive and are not accessible for most researchers.

On the other hand, the last few years have shown also a steady improvement in X-ray source technology so that now inexpensive compact sealed X-ray microfocus tubes can be produced with a very long lifetime. At this moment, the attainable spot size is of the order of 5 micrometer but with the steady technological improvement one can expect submicron X-ray sources in the coming years.

3.4. Characterisation (SEM) of the microstructure of the cement paste – cement paste components and hydration degree

The pore structure and phase composition [23] of the samples can be also be measured on polished sections using a scanning electron microscope (SEM). The samples are firstly impregnated under vacuum with a fluid epoxy before polishing. The images are obtained on these polished sections (5×3 cm) with a SEM using a solid state Back-Scattered Electron detector (BSE). Backscattering is defined as the deflection of the electrons by the scattering process through an angle $> 90°$ relative to the incident direction. These electrons provide a signal that is atomic-number dependent. The atomic-number dependence of Back-Scattered electron Imaging (BEI) can be used as the basis of a micro-analytical technique as it provides a sensitive discrimination between the different phases of the specimen. This is illustrated in Fig. 7.

Chemical Image mappings are images based on the information recorded and digitised from Energy-Dispersive X-Ray analysis (EDX) detectors. These detectors discriminate X-Ray energies emitted from the sample and are capable of performing analysis of elements beginning with boron in the periodic table. The Chemical Image maps are merely digital images that use the X-Ray signal to carry compositional information. Each pixel contains the number of X-rays counts. At present image analysis equipment can provide the means to combine quantitative BEI with chemical image mappings.

The following components of the cement paste can easily be identified:

- Anhydrous Cement,
- Calcium Hydroxide,
- Hydration Products,
- Pores and cracks.

The measured area fraction of these four phases is equal to the volume fraction of the phase in the cement paste sample if the structure is uniform, isotropic and random.

This method can thus be used to determine the hydration degree of the cement paste.

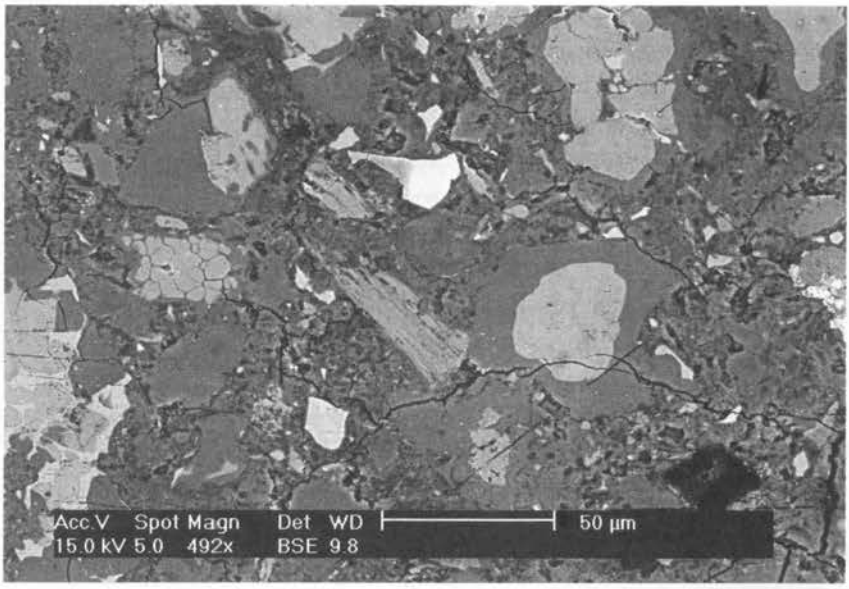

FIGURE 7. BSE-image of a polished sample of cement paste showing the hydration products as a grey rim around the non-hydrated cement mineral phases. The pores and cracks are colored dark-grey to black.

Acknowledgement

This article is related to research carried out in the framework of EC funded research projects under the contracts BREU-CT91-0490 and SMT4-CT95-2006.

References

1. IUPAC Manual of Symbols and Terminology, Appendix 2, Pt.1, *Colloid and Surface Chemistry, Pure Appl. Chem.*, Vol.31, p.578, 1972.

2. L. STRUBLE and P. STUTZMAN, *Epoxy Impregnation of Hardened Cement for Microstructural Characterisation*, NBSIR 88-3702-1989.

3. P. STUZMAN, *Serial Sectioning of Hardened Cement Paste for Scanning Electron Microscopy*, NISTIR 90-4235-March 1990.

4. N. THAULOW, A.D. JENSEN, S. CHATTERJI, P. CHRISTENSEN, and H. GUDMUNDSSON, Estimation of the compressive strength of concrete samples by means of fluorescence microscopy, Nordisk Betong, Vol.2-4, pp.51-52, 1982.

5. A.D. JENSEN, K. ERIKSEN, S. CHATTERJI, N. THAULOW, and I. BRANDT, *Petrographic Analysis of Concrete*, Special Publication of the Danish Building Export Council, Copenhagen.

6. B. MAYFIELD, The quantitative evaluation of the water/cement ratio using fluorescence microscopy, *Magazine of Concrete Research*, Vol.42, No.150, pp.45-49, 1990.

7. S. WIRGOT and F. VAN CAUWELAERT, The measurement of impregnated cement paste fluorescence by means of image analysis, *Proceedings of the Third Euroseminar on Microscopy applied to Building Materials*, Barcelona, September 1991.

8. J. ELSEN, N. LENS, J. VYNCKE, T. AARRE, D. QUENARD, and V. SMOLEJ, Determination of the w/c ratio of hardened cement paste and concrete samples on thin sections using automated image analysis techniques, *Cement and Concrete Research*, Vol.25, No.4, pp.827-843, 1995.

9. J.S. PLOEM and H.J. TANKE, Introduction to fluorescence microscopy, *Microscopy Handbooks*, Vol.10, Royal Microscopical Society, 1987.

10. J. ELSEN, Automated air void analysis on hardened concrete, results of a European intercomparison testing programme, *Cement and Concrete Research*, Vol.31, pp.1027-1031, 2001.

11. T.C. POWERS, The air requirement of frost resistant concrete, Proceedings, *Highway Research Board*, Vol.29, pp.184-202, 1949.

12. A. SCHÄFER, Frostwiderstand und Porengefüge des Betons. Beziehungen und Prüfverfahren, *Deutscher Ausschuss für Stahlbeton*, No.167, 1964.

13. T.C. POWERS, Freezing effects in concrete, in: *Durability of Concrete, Special Publication SP-47*, American Concrete Institute, pp.1-11, 1975.

14. P. PLANTE, M. PIGEON, F. SAUCIER, Air void stability, part V: Temperature, general analysis, and performance index, *ACI Materials Journal*, Vol.88, pp.25-30, 1991.

15. J. ELSEN, N. LENS, J. VYNCKE, T. AARRE, D. QUENARD, V. SMOLEJ, Quality assurance and quality control of air entrained concrete, *Cem. Con. Res.*, Vol.24, No.7, pp.1267-1276, 1994.

16. B.W. LANGAN, M.A. WARD, Determination of the air-void system parameters in hardened concrete – an error analysis, *ACI Materials Journal*, Vol.83, No.6, pp.943-953, 1986.

17. R. PLEAU, P. PLANTE, R. GAGNE, M. PIGEON, Practical considerations pertaining to the microscopical determination of air void characteristics of hardened concrete (ASTM C457 standard), *Cem. Con. Aggreg.*, Vol.12, No.2, pp.3-11, 1990.

18. H. SOMMER, The precision of the microscopical determination of the air-void system in hardened concrete, *Cem. Con. Aggreg.*, Vol.1, No.2, pp.49-55, 1979.

19. M. SANDSTRÖM, Air void distribution in concrete, *Proceedings of the 3rd Euroseminar on Microscopy Applied to Building Materials*, Barcelona, September 1991.

20. B. SCHOUENBORG, J.E. LINDQVIST, M. SANDSTRÖM, *Air and Air Void Structures in Concrete – General Overview and Picture Atlas*, Nordtest Project 1121-93, Published by the Swedish National Testing and Research Institute, SP-report 1995:51, BORÅS, 1995.

21. T. OHTA, *Transactions of the Japan Concrete Institute*, Vol.8, pp.183-190, 1986.

22. A. SASOV, D. VAN DYCK, Desktop X-ray microscopy and microtomography, *Journal of Microscopy*, Vol.191, pp.151-158, 1998.

23. B.W. ROBINSON and E.H. NICKEL, A useful new technique for mineralogy: the backscattered-electron / low vacuum mode of SEM operation, *Am. Mineralogist.*, Vol.64, pp.1322-1328, 1979.